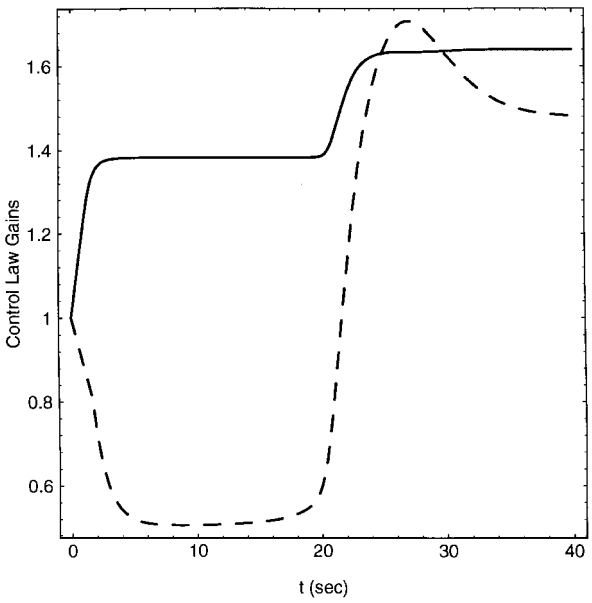

Fig. 3 Adaptive-control-law gains, $\kappa_1(0) = \kappa_2(0) = 1$, $\tau_1 = \tau_2 = 1$ (——, κ_1, and - - -, κ_2).

and flight-path angle ψ of 10 deg. The initial lander velocity is set at 5 m/s to represent residual errors from the previous descent phase. It is assumed that the lander uses clustered descent thrusters and that a set of these thrusters fails with the throttle open, inducing a constant-bias acceleration of $0.5g$. In addition, at the midpoint of the descent maneuver, the remaining thrusters are degraded with the available thrust reduced to one-third of the initial available thrust. This failure mode is modeled by multiplying the commanded thrust by

$$f(t) = \tfrac{2}{3}\left[1 - (1/\pi)\tan^{-1}(2t - t_f)\right] \tag{10}$$

so that the actuated thrust weight ratio becomes $\tilde{n}(v, h) f(t)$.

The descent profile of the lander is shown in Figs. 2a and 2b along with the commanded and actuated thrust weight ratio. It can be seen that the initial velocity error is removed by throttling down the descent thrusters to allow the lander to accelerate and, finally, to track the required descent profile, even in the presence of the 0.5-g bias acceleration. Then, at the midpoint of the maneuver, the available thrust is reduced, as described above. It can be seen from Fig. 3 that the control-law gains adapt to this failure and that after a short transient the lander continues to accurately track the required descent profile. This failure is compensated for by increased demands on the remaining descent thrusters, as seen in Fig. 2b. On landing, the actuated thrust weight ratio is only 0.5 because of the jammed thrusters providing a constant $0.5g$ bias acceleration. Therefore, the lander has a total thrust/weight ratio of unity, as required for a soft landing. It is also found that $\psi \to 0$, so that a vertical landing is ensured.

VI. Conclusions

A direct adaptive control law for gravity-turn descent is presented that is robust and able to compensate for multiple thruster failures. The control-law gains adapt to these failures in direct response to the changing behavior of the system dynamics. Because on-line parameter estimation is not required, the control law is computationally efficient for onboard implementation. Such robust and efficient control laws appear attractive for low-cost planetary or lunar landers, where high controller performance is required, but without significant computational effort.

References

[1]Cheng, R. K., "Lunar Terminal Guidance," *Lunar Missions and Exploration*, edited by C. T. Leondes and R. W. Vance, Wiley, New York, 1964, pp. 308–355.

[2]Citron, S. J., Dunn, S. E., and Meissinger, H. F., "A Terminal Guidance Technique for Lunar Landing," *AIAA Journal*, Vol. 2, No. 3, 1964, pp. 503–509.

[3]Cheng, R. K., "Terminal Guidance for a Mars Softlander," 8th International Symposium on Space Technology and Science, Tokyo, Japan, 1969, pp. 855–865.

[4]McInnes, C. R., "Gravity Turn Descent with Quadratic Air Drag," *Journal of Guidance, Control, and Dynamics*, Vol. 20, No. 2, 1997, pp. 393, 394.

[5]Cheng, R. K., "Design Consideration for Surveyor Guidance," *Journal of Spacecraft and Rockets*, Vol. 3, No. 11, 1966, pp. 1569–1576.

[6]Ingoldby, R. N., "Guidance and Control System Design of the Viking Planetary Lander," *Journal of Guidance and Control*, Vol. 1, No. 3, 1978, pp. 189–196.

[7]McInnes, C. R., "Non-Linear Transformation Methods for Gravity-Turn Descent," *Journal of Guidance, Control, and Dynamics*, Vol. 19, No. 1, 1996, pp. 247, 248.

[8]Hong, J., Bhat, S. P., and Bernstein, D. S., "Adaptive Nonlinear Motion Control," Aerospace Engineering Dept. Internal Rept., Univ. of Michigan, Ann Arbor, MI, March 1998.

[9]McInnes, C. R., "Terminal Descent to the Lunar Surface with Terrain Constraints," *Acta Astronautica*, Vol. 36, No. 7, 1995, pp. 367–377.

Propulsion System Sizing for Orbital Inspection Vehicles

Trevor Williams*
University of Cincinnati, Cincinnati, Ohio 45221
and
Sergei Tanygin†
Analytical Graphics, Inc., Malvern, Pennsylvania 19355

Introduction

THERE is currently growing interest in the development of remotely piloted inspection vehicles capable of performing fly-arounds of the Space Shuttle or of a space station on-orbit. For example, NASA flight tested the AERcam, the autonomous extravehicular activity robotic camera Sprint vehicle[1,2] that is the prototype of a family of spacecraft for Shuttle and International Space Station inspection tasks, during the recent STS-87 mission. This Note describes methods for selecting the two main parameters that describe the propulsion system of such vehicles: the total Δv capacity of the tankage and the thrust level of the jets. Δv requirements are clearly related to the desired mission range and flight duration, as well as attitude control requirements. Choice of thrust level must be made on the basis of a tradeoff between safety and performance, bearing in mind the types of missions to be performed by such a vehicle. As regards safety, too high a thrust may pose unacceptable risks of a high-speed collision in the event that a malfunction on the inspection vehicle causes it to fire toward the mother spacecraft. For instance, if a thruster becomes stuck on, the resulting long-term net linear acceleration may, in some cases,[3] approach the one-jet thrust/mass ratio of the vehicle. On the other hand, too low a thrust level will not permit the vehicle to overcome orbital effects and hover at an appreciable distance above, below, or to the side of the larger spacecraft; such positioning is likely to prove very desirable in future inspection missions.

The safety issues given in the preceding points dictate that inspection vehicles will necessarily be low-thrust spacecraft: accelerations as low 50 μg have been considered.[4] Consequently, extended burns will be required to accelerate up to even moderate relative speeds. The usual assumption of an impulsive Δv is, thus, not valid for this class of spacecraft. Furthermore, these vehicles are initially to be flown by a human operator, essentially by means of visual cues alone. Therefore, low-thrust optimal control techniques that require

Received Jan. 15, 1997; revision received Aug. 17, 1998; accepted for publication Sept. 24, 1998.

*Associate Professor, Department of Aerospace Engineering. Associate Fellow AIAA.

†Senior Astro-Development Engineer, 325 Technology Drive.

continuous attitude maneuvering (see, for instance, Ref. 5) cannot realistically be applied to this problem. Instead, maneuvers will be assumed here to be carried out by performing an acceleration burn at a fixed attitude, then coasting, and then performing a deceleration burn at some other fixed attitude. Questions that are of practical interest include how the vehicle acceleration level affects the maximum transfer distance that is achievable in a given time, and how it affects the total Δv, i.e., propellant, that is required for the transfer.

This analysis is based on the Clohessy–Wiltshire equations that describe the relative motion of two spacecraft in close orbits.[6] The usual closed-form coasting solutions to these equations are first modified to include a constant acceleration input. These solutions then permit computation of the thrusting time and direction required to achieve a desired final velocity vector, in the presence of orbital effects, for different vehicle accelerations. These times in turn allow acceleration/coast/deceleration (ACD) trajectories to be derived, as functions of thrust level, which transfer the vehicle from rest at one position to rest at some other specified location after a given total transfer time. Rest-to-rest maneuvers are considered because, if the spacecraft has a nonzero velocity when it arrives at the target, it typically overshoots this point considerably while attempting to then execute a prolonged low-acceleration braking burn. A second attractive feature of rest-to-rest transfers is that quite complicated mission profiles can be built up as a combination of rest-to-rest transfers between a sequence of waypoints. Each leg of this type of mission can be analyzed independently of all others, as each begins and ends with the same (zero) velocity. One conclusion from this analysis that is of practical significance is that appreciable total Δv, e.g., 20%, can be saved by avoiding unduly low values for vehicle acceleration. This results from orbital effects being able to overwhelm the acceleration produced by very small thrusters, thus leading to inefficient maneuvers. Increasing thrust somewhat allows shorter burns to be used to achieve the same relative velocity, therefore coming closer to the ideal case of an impulsive Δv.

Problem Formulation

The motion of an object relative to another in a nearby circular reference orbit of angular rate ω is described by the Clohessy–Wiltshire (CW) equations.[6] In the local vertical/local horizontal (LVLH) coordinate system that is normally used to describe on-orbit proximity operations, these become

$$\ddot{x} - 2\omega\dot{z} = a_x, \qquad \ddot{y} + \omega^2 y = a_y, \qquad \ddot{z} - 3\omega^2 z + 2\omega\dot{x} = a_z \tag{1}$$

where the x axis is directed along the velocity vector (or VBAR) of the reference body, the z axis along the downward local vertical (or RBAR), and the y axis along the orbit normal. Note that the equation in y is decoupled from those in x and z; it represents simple harmonic motion out of the orbital plane. These equations have closed-form solutions[7] for the unforced case $a_x = a_y = a_z = 0$, which can be used to determine the coasting motion that results from a known initial velocity. They can also be differentiated to give closed-form velocity expressions. Finally, they can also be used to compute the magnitude and direction of the initial velocity that is required to transfer from a given position to a desired one in a specified time. This property makes them extremely useful for vehicles with sufficiently high thrust that velocity changes can be made impulsively, i.e., essentially instantaneously. (For an application to the development of rendezvous trajectories for rescue of an astronaut who becomes separated from a space station, see Ref. 8.) These *CW targeting* equations decouple into a (2×2) in-plane (IP) system and a scalar out-of-plane (OOP) equation. However, these equations cannot be used for low-thrust vehicles as considered here. The low-thrust case is the subject of the next section.

Main Results

The equations of motion for a low-thrust IP rest-to-rest ACD maneuver are given by the first and third components of Eq. (1), with applied acceleration:

$$(a_x, a_z) = \begin{cases} (a\cos\theta, -a\sin\theta), & 0 \le t \le t_1 \\ (0, 0), & t_1 < t \le t_2 \\ (a\cos\phi, -a\sin\phi), & t_2 < t \le \tau \end{cases} \tag{2}$$

This corresponds to holding the direction of thrust fixed in the rotating LVLH frame throughout the acceleration phase and again during the braking phase. An alternative approach that was also investigated was to thrust along directions that were fixed inertially. However, this variant was observed to give results that were inferior to those obtained by means of LVLH-fixed thrusting. Furthermore, it does not allow visual cues, e.g., the line of sight to the horizon of the Earth, to be used for thrust steering.

The boundary conditions for the maneuver are $[x(0), z(0)] = (x_0, z_0)$ and $[x(\tau), z(\tau)] = (x_\tau, z_\tau)$ on position and $[\dot{x}(0), \dot{z}(0)] = [\dot{x}(\tau), \dot{z}(\tau)] = (0, 0)$ on velocity, with total transfer time τ. The first question is to ascertain whether a transfer is even feasible for the specified values for a and τ. If it is, then the maneuver can be defined completely by determining the required transition times t_1 and t_2 and thrust angles θ and ϕ. The first step in calculating this solution is to derive the closed-form solutions to the IP CW equations in the presence of thrusting. If we consider a maneuver leg that starts at position (x_0, z_0) and velocity $(\dot{x}_0, \dot{z}_0)$ during which the LVLH acceleration components are held constant at (a_x, a_z), then the resulting position at time t can be shown to be given as

$$\begin{aligned} x(t) = \Big\{ & -2(\dot{z}_0 + 2a_x/\omega)\cos\omega t + [4(\dot{x}_0 - a_z/2\omega) \\ & - 6\omega z_0]\sin\omega t - \tfrac{3}{2}a_x\omega t^2 + [6\omega z_0 - 3(\dot{x}_0 - a_z/2\omega) \\ & + a_z/2\omega]\omega t + [\omega x_0 + 2(\dot{z}_0 + 2a_x/\omega)]\Big\}\Big/\omega \end{aligned} \tag{3}$$

and

$$\begin{aligned} z(t) = & \{[2(\dot{x}_0 - a_z/2\omega) - 3\omega z_0]\cos\omega t + [\dot{z}_0 + 2a_x/\omega]\sin\omega t \\ & - 2a_x t + [4\omega z_0 - 2(\dot{x}_0 - a_z/2\omega)]\}/\omega \end{aligned} \tag{4}$$

(These expressions reduce to the standard CW solutions if $a_x = a_z = 0$.)

Just as the closed-form CW solutions in the thrust-free case lead to the impulsive CW targeting, so, too, do Eqs. (3) and (4) give rise to a technique for maneuvering between two given points in a specified time by means of a constant thrust. If the desired transfer is from position (x_0, z_0) and velocity $(\dot{x}_0, \dot{z}_0)$ to position (x_τ, z_τ) (velocity unspecified) in time τ, then it can be shown that the required acceleration components are given as the solution of the simultaneous equations

$$\begin{pmatrix} \lambda & \mu \\ -\mu & \nu \end{pmatrix} \begin{pmatrix} a_x \\ a_z \end{pmatrix} = \begin{pmatrix} \hat{x} \\ \hat{z} \end{pmatrix} \tag{5}$$

where the three matrix elements

$$\lambda = \frac{\left(4[1 - \cos\omega\tau] - \tfrac{3}{2}\omega^2\tau^2\right)}{\omega^2}$$
$$\mu = \frac{2(\omega\tau - \sin\omega\tau)}{\omega^2}, \qquad \nu = \frac{(1 - \cos\omega\tau)}{\omega^2} \tag{6}$$

and the two vector entries

$$\begin{aligned} \hat{x} = {} & x_\tau - x_0 - (2\dot{z}_0/\omega)[1 - \cos\omega\tau] - 6z_0[\omega\tau - \sin\omega\tau] \\ & - (4\dot{x}_0/\omega)\sin\omega\tau + 3\dot{x}_0\tau \\ \hat{z} = {} & z_\tau - 4z_0 + (2\dot{x}_0/\omega)[1 - \cos\omega\tau] \\ & + 3z_0\cos\omega\tau - (\dot{z}_0/\omega)\sin\omega\tau \end{aligned} \tag{7}$$

depend entirely on known quantities. Similar expressions can also be developed for the acceleration components required in order to take the spacecraft from given initial conditions to a specified velocity $(\dot{x}_\tau, \dot{z}_\tau)$ (position unspecified) in time τ. In both of these versions, the required acceleration magnitude $a = \sqrt{(a_x^2 + a_z^2)}$ typically decreases monotonically as transfer time increases. A numerical interpolation procedure can then be used to determine the value for τ that corresponds to any given acceleration level a. This then forms the basis for the following iterative procedure for generating IP rest-to-rest ACD trajectories:

1) Use standard CW targeting to find the impulsive Δv_1 required to initiate a transfer of total time τ, and the braking Δv_2 (the negative of the final velocity) required to come to rest impulsively at the target.

2) Use the velocity equivalents of Eqs. (5–7) to determine the time t_1 and thrust direction θ that would be required to apply Δv_1 by means of continuous thrusting at the specified acceleration level a. This in turn defines, by Eqs. (3) and (4), the position at the end of this acceleration leg.

3) Perform a similar procedure, but in negative time, to determine the time t_2 and thrust direction ϕ required for a continuous-thrust deceleration leg that brings the vehicle to rest at the target from an initial velocity of $-\Delta v_2$. The position at the start of this leg can then also be found by applying Eqs. (3) and (4) in negative time.

4) Return to step 1 to compute a new impulsive transfer, but now using the end of the acceleration burn as the initial point, the start of the deceleration burn as the final point, and $\tau - t_1 - t_2$ as the transfer time. This reflects that the Δv are not instantaneous.

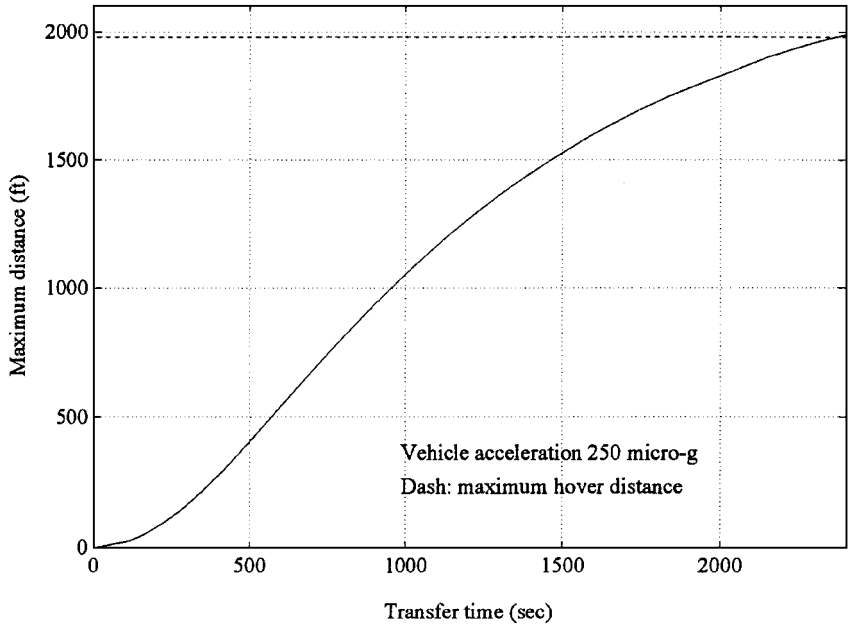

Fig. 1 Maximum achievable distance along RBAR.

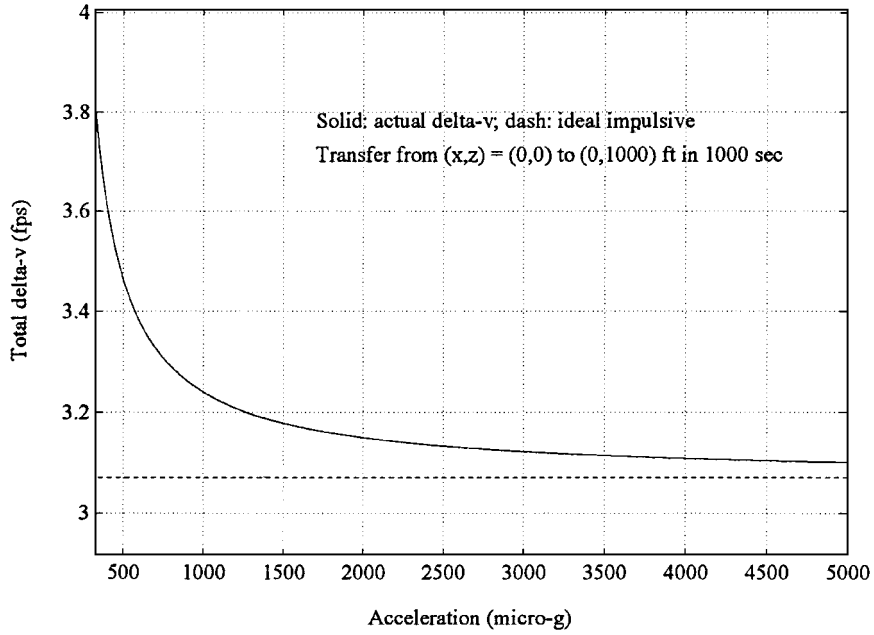

Fig. 2 Total RBAR maneuver Δv vs impulsive.

5) Repeat until sufficiently converged.

One complication of IP orbital motion is that the results obtained depend not only on the distance traveled, but also on the direction. In particular, results for translations along the VBAR (the easiest direction to translate along) are significantly different from those for RBAR transfers. However, both the IP and OOP results can be used to quantify the maximum range that is achievable in a given time for a specified acceleration level, by considering transfers with zero-length coast phases. Similarly, they can be used to examine the effect of increasing acceleration level on the total maneuver Δv for transfers between two specified points in a given time. Results will be presented here for IP transfers from the origin to a point along the positive RBAR; the corresponding results for VBAR and OOP transfers are given in Ref. 9.

The maximum distance achievable for transfers along the RBAR is given in Fig. 1. It can be shown to be considerably less than the corresponding distances for transfers along the other two axes; this reflects the difficulty of maneuvering along the RBAR. This difficulty is also demonstrated by the relatively small maximum hover distance, or RBAR hover limit [the maximum radial distance at which the spacecraft is able to station keep by thrusting constantly; from Eq. (1), this distance is $z_h = a/3\omega^2$] of just under 2000 ft for an acceleration of 250 μg. Figure 2 then shows how the maximum maneuver Δv depends on vehicle acceleration; the dashed line in this case shows the value obtained by the standard CW targeting equations for an impulsive vehicle. It can be seen that increasing vehicle acceleration from 250 to 2500 μg leads to a reduction in total maneuver Δv of around 20%; this reduction in the maneuver propellant requirement is quite significant.

Conclusions

This Note has studied low-thrust proximity operations of the type arising with the new class of orbital inspection vehicles. Closed-form expressions were first derived for the trajectory of a spacecraft that is acted upon by a continuous thrust. These were then used as the basis for a numerical procedure for generating a rest-to-rest ACD trajectory that takes a vehicle with a specified acceleration level between two desired points in a specified time. This analysis leads to the following main conclusion: increasing vehicle acceleration by an order of magnitude above the theoretical minimum leads to significantly reduced propellant consumption.

References

[1]"AERCam Sprint Flight Test Project Critical Design Review," NASA Johnson Space Center Automation, Robotics, and Simulation Div., July 1996.

[2]Williams, T. W., and Tanygin, S., "On-Orbit Engineering Tests of the AERCam Sprint Robotic Camera Vehicle," *Proceedings of the AAS/AIAA Spaceflight Mechanics Meeting* (Monterey, CA), Univelt, San Diego, CA, 1998 (American Astronautical Society Paper AAS 98-171, Feb. 1998).

[3]Williams, T. W., and Tanygin, S., "Dynamics of a Near-Symmetrical Spacecraft Driven by a Constant Thrust," *Proceedings of the AAS/AIAA Spaceflight Mechanics Meeting* (Austin, TX), Univelt, San Diego, CA, 1996 (American Astronautical Society Paper AAS 96-160, Feb. 1996).

[4]"Inspector Project Summary," NASA Johnson Space Center Automation, Robotics, and Simulation Div., Aug. 1995.

[5]Kechichian, J. A., "Reformulation of Edelbaum's Low-Thrust Transfer Problem Using Optimal Control Theory," *Journal of Guidance, Control, and Dynamics*, Vol. 20, No. 5, 1997, pp. 988–994.

[6]Clohessy, W. H., and Wiltshire, R. S., "Terminal Guidance System for Satellite Rendezvous," *Journal of the Aerospace Sciences*, Vol. 27, 1960, pp. 653–658.

[7]Kaplan, M. H., *Modern Spacecraft Dynamics and Control*, Wiley, New York, 1976.

[8]Jensen, M. C., Hines, J. M., and Foale, C. M., "Man Overboard Rescue," *Simulation*, Vol. 57, 1991, pp. 39–47.

[9]Williams, T. W., and Tanygin, S., "Trajectory Issues Affecting Propulsion System Sizing and Operations of Orbital Inspection Vehicles," *Proceedings of the AIAA/AAS Astrodynamics Conference* (San Diego, CA), CP969, AIAA, Reston, VA, 1996, pp. 686–696.

Closed-Form Methods for Generating On–Off Commands for Undamped Flexible Spacecraft

William E. Singhose*
Georgia Institute of Technology, Atlanta, Georgia 30332
and
Bart W. Mills† and Warren P. Seering‡
Massachusetts Institute of Technology, Cambridge, Massachusetts 02139

I. Introduction

SEVERAL methods for generating command profiles for flexible spacecraft have recently been proposed.[1–7] Many of these techniques have been directed toward systems equipped with on–off reaction jets. Using the commands generated by these methods, a flexible spacecraft can be moved with small levels of residual vibration. Furthermore, the commands can be robust to modeling errors,[2,4,8] limit transient deflection,[5] and limit fuel consumption.[6] Although these techniques are powerful, they have the drawback that a separate numerical optimization must be performed to generate the command for every unique motion. This drawback introduces a time delay at the start of every motion, or requires the command profiles to be precomputed and stored for retrieval.

Consider rest-to-rest slewing of a two-mass and spring system where the control force acts on the first mass m_1. To account for the case of on–off actuators, the force is restricted to values of $u_{\max}$, 0, and $-u_{\max}$. If all system parameters (m_1, m_2, k, $u_{\max}$) are set equal to 1, then the system has a natural frequency of $\sqrt{2}$ rad/s and a force-to-mass ratio of 0.5.

Designing a bang-bang command profile (the simplest on–off command) to move the benchmark system, a desired distance is straightforward. If we assume that the bang-bang command begins at time zero, then the only unknown is the switch time t_2 because the duration of the negative pulse must equal the duration of the positive pulse to bring the system to rest. The value of t_2 can be obtained from the rigid-body dynamics as

$$t_2 = \sqrt{x_d/\alpha} \tag{1}$$

where x_d is the desired move distance and $\alpha = u_{\max}/(m_1 + m_2)$ is the force-to-mass ratio. The bang-bang command moves the center of mass to the desired position, but significant residual oscillations will usually exist when the system has flexibility. However, the bang-bang command has the advantage of being completely described by the simple expression given in Eq. (1).

By taking into account the system flexibility, time-optimal and near time-optimal command profiles can be generated to eliminate the residual vibration.[1–6,8] The time-optimal open-loop command profiles for linear systems are multiswitch bang-bang commands that must be obtained using a numerical optimization. The rise time is slower than with the bang-bang command, but the residual oscillation is eliminated. The development of time-optimal flexible-body commands will not be explained here, but we emphasize that

Received Oct. 23, 1997; revision received Oct. 18, 1998; accepted for publication Oct. 30, 1998.

*Assistant Professor, Department of Mechanical Engineering. Member AIAA.

†Research Assistant, Department of Mechanical Engineering.

‡Professor, Department of Mechanical Engineering.